IPPJ-AM-23

DIELECTRONIC RECOMBINATION OF HYDROGENIC IONS

T.FUJIMOTO, T.KATO AND Y.NAKAMURA

INSTITUTE OF PLASMA PHYSICS
NAGOYA UNIVERSITY

NAGOYA, JAPAN

IPPJ-AM-23

DIELECTRONIC RECOMBINATION OF HYDROGENIC IONS

Takashi Fujimoto[1], Takako Kato and Yukiharu Nakamura[2]

Institute of Plasma Physics, Nagoya University
Chikusa-ku, Nagoya 464, Japan

August 1982

Parmanent address:

1) Department of Engineering Science, Faculty of Engineering, Kyoto University
2) Japan Atomic Eiiergy Research Institute

Abstract

Various approximate formulas for total or overall dielectronic recombination rate coefficient are compared with detailed calculations for the case of recombination of hydrogenic ion to helium-like ion. The revised version of the general formula by Burgess(1976) agrees well with the calculations by Dubau(1973), Dubau et.al.(1981) or Fujimoto and Kato(1981). The limiting case of infinite nuclear charge and the effect of the finite plasma density are also discussed.

§1. Introduction

For high-temperature plasmas like the solar corona, tokamak plasmas etc., dielectronic recombination [1,2] is an important recombination mechanism for ions. This process consists of the two-step transitions involving doubly excited states lying in the continuum states. i.e. dielectronic capture and stabilizing transition, and the calculation of the recombination rate coefficient may accordingly be complicated. This difficulty stems partly from our insufficient knowledge of the doubly excited state and especially of its autoionization probability from these states.

To meet the practical requirements to estimate the total dielectronic recombination rate coefficient, several semi-empirical formulas or approximate formulas have been proposed that are based on various assumptions and approximations for individual processes involved. Agreement among these formulas, however, is generally not satisfactory. Furthermore, various new processes that affects the recombination rate are being proposed from time to time. Therefore, it does not appear that we have reached the point where we can predict the overall or total recombination rate for various ions with a reasonable reliability.

For the simplest case of ions with only two electrons, the problem should be much easier to handle: i.e. dielectronic recombination from a hydrogenic ion to a helium-like ion. This is because we have fairly ample information, theoretical and experimental, of these doubly excited states of helium-like ions. For instance, observaiton of helium-like satellite lines associated with hydrogen-like resonance-series lines is one of the most important sources of our knowledge. There are numerous theoretical calculations, too. Using such information we are able to calculate an individual dielectronic recombination rate coefficient that describes a process via a doubly excited level to reach an individual normal excited state of helium-like ion. Then, these individual rate coefficients are summed over all of the normal levels to result in a total dielectronic recombination rate coefficient.

In the following we treat the total dielectronic recombination rate coefficient of hydrogenic ions to helium-like ions; we compare various formulas so far proposed, and we try to assess the reliability of these formulas by comparing these with a detailed calculations where possible. We also discuss the limiting case of the infinite nuclear charge and examine the effect of finite electron and ion densities on the dielectronic recombination; the latter problem should be important when the plasma has a high density as is the case for the laser-produced plasma. We hope this report would serve as a basis for further study of ions other than hydrogenic.

§ 2. Dielectronic recombination*

We consider the schematic energy level diagram of Fig.1 pertinent to dielectronic recombination. Let $X_z(j)$ denote the normal state j of z-times ionized ion, where g corresponds to the ground state, and $X_{z-1}(j,n\ell')$ the state with the "core" electron j and the "running" electron $n\ell'$, where n and ℓ' are, respectively, the principal and angular-momentum quantum numbers. $E_{g,j}$ is the excitation energy of state j and ΔE is that for the state $(j,n\ell')$. A_a denotes the autoionization probability and r_d is its inverse dielectronic capture probability. A_r is the stabilizing transition probability. The process of dielectronic recombination is represented by

$$X_z(g) + e \underset{(A_a)}{\overset{(r_d)}{\rightleftarrows}} X_{z-1}(j,n\ell') \xrightarrow{(A_r)} X_{z-1}(g,n\ell') + h\nu'. \qquad (1)$$

If we express the dielectronic capture rate coefficient r_d in terms of its cross section σ_d we have the balance relation for the population density of the state $X_{z-1}(j,n\ell')$

$$n_z(g)n_e f(\Delta E)v\sigma_d(j,n\ell')\delta E = n_{z-1}(j,n\ell')[A_r(j,n\ell') + A_a(j,n\ell')], \qquad (2)$$

*This section is based primarily on the trearment of ref.3.

where $n_z(g)$ is the density of the ion $X_z(g)$ and n_e is the electron density with the velocity (v) distribution f(E) and we assign the energy width δE to the state $(j,n\ell')$. In the limit of small stabilizing transition probability $A_r(j,n\ell')$ we have the LTE or Saha population for $(j,n\ell')$

$$\frac{n_{z-1}(j,n\ell')}{n_z(g)n_e} = Z_{j,n\ell'}$$

$$\equiv \frac{\omega_{z-1}(j,n\ell')}{2\omega_z(g)} \left(\frac{h^2}{2\pi mkT_e}\right)^{3/2} e^{-\Delta E/kT_e} , \tag{3}$$

where we have assumed the Maxwellian distribution for the electrons having the electron temperature T_e,

$$f(E)dE = \sqrt{\frac{2m}{\pi}} \frac{v}{(kT_e)^{3/2}} e^{-E/kTe} dE. \tag{4}$$

Here ω denotes the statistical weight, h is the Planck constant and k is the Boltzmann constant. Thus, we obtain the relation for the case of $A_a \gg A_r$

$$A_a(j,n\ell') = Z^{-1}_{j,n\ell'} f(\Delta E)v\sigma_d(j,n\ell')\delta E$$

$$= \frac{8\pi m^2 v^2}{h^3} \frac{\omega_z(g)}{\omega_{z-1}(j,n\ell')} \sigma_d \delta E \tag{5}$$

In the general case of $A_r \neq 0$. we have

$$n_{z-1}(j,n\ell') = \frac{1}{A_r + A_a} n_z(g) n_e f(\Delta E) v \sigma_d \delta E$$

$$= Z_{j,n\ell'} \frac{A_a}{A_r + A_a} n_z(g) n_e \ , \qquad (6)$$

where use has been made of eq. (5). Sometimes the quantity $A_a(j,n\ell')/[A_r(j,n\ell') + A_a(j,n\ell')]$ is represented as $b(j,n\ell')$. The dielectronic recombination rate coefficient for an individual level $X_{z-1}(g,n\ell')$ is given as

$$\alpha_d(g,n\ell') = \frac{1}{n_z(g) n_e} \sum_j n_{z-1}(j,n\ell') A_r(j,n\ell' \rightarrow g,n\ell')$$

$$= \sum_j Z_{j,n\ell'} \frac{A_a A_r}{A_a + A_r}$$

$$= \left(\frac{h^2}{2\pi m k T_e} \right)^{3/2} \sum_j \frac{\omega_{z-1}(j,n\ell')}{2\omega_z(g)} \frac{A_r}{1 + A_r/A_a} e^{-\Delta E/kT_e}. \qquad (7)$$

By taking the sum over all the excited states $X_{z-1}(g,n\ell')$ we obtain the total or overall recombination rate coefficient

$$\alpha_d^{tot} = \sum_{n,\ell'} \alpha_d(g,n\ell') \ . \qquad (8)$$

We note the relation between the excitation cross section, σ_{ex} for $X_z(g) + e \longrightarrow X_z(j) + e$, and the dielectronic capture rate coefficient or autoionization probability. The quantum-defect theory shows that the partial excitation cross section corresponding to the angular momentum ℓ' for the outgoing electron continues smoothly across the limit $E_{g,j}$ down to the dielectronic capture cross section to the doubly excited states

$$\sigma^{z}_{ex}(g \longrightarrow j,\ell')dE = \overline{\sigma_d (g \rightarrow j,n\ell')\delta E}\ dn \ . \qquad (9)$$

Figure 2 depicts schematically the situation, where the energy "position" of the doubly excited states is represented by a triangle with the width δE. Equation (9) is further transformed as

$$\sigma_d(g \longrightarrow j,n\ell')\delta E = \sigma^{z}_{ex}\ (g \longrightarrow j,\ell')\ \frac{dE}{dn}$$

$$= \frac{2z^2}{n^3}\, I_H\, \sigma^{z}_{ex}\ (g \longrightarrow j,\ell'), \qquad (9')$$

where I_H is one Rydberg (13.6 eV). Thus, with the help of eq.(5) we may express the autoionization probability as the extrapolation of the excitation cross section

$$A_a(j,n\ell') = \frac{4z^2\Delta E}{h\ n^3}\ \frac{\omega_z(g)}{\omega_{z-1}(j,n\ell')}\ \frac{\sigma^{z}_{ex}\ (g \longrightarrow j,\ell')}{\pi a_0^2} \qquad (10)$$

$$= \frac{4}{h\ n^3}\ \frac{I_H}{\omega_{z-1}(j,n\ell')}\ z^2\, \Omega\,(g \longrightarrow j,\ell') \qquad (10')$$

where $\Omega(g \longrightarrow j,\ell')$ is the partial-wave collision strength of the excitation.

In eq.(1), we have assumed that the doubly excited level $(j, n\ell')$ has only one autoionization channel leaving the ion in the ground state g. However, it may have another channel in which it autoionizes into an excited level, say i, of the ion. Then, equation (7) should be accordingly modified. Jacobs et al,[4], have pointed out its significance, and its effect has been included in their calculation. Its effect has been found to be significant for some cases (e.g., F-like ions).

The above mechanism corresponds to the resonance contribution to the excitation cross section $g \longrightarrow i$ of the ion. Its effect has been proposed in ref. 5) and has been evaluated[6] for hydrogenic ions. It has been found that its contribution is about 10%.

Since the effect of the above channel is not expected to be too important in our case, we neglect it throughout in the following discussion.

§ 3. Various formulas

3.1. Burgess' general formula[1)]

We define the average autoionization probability for the (j, nℓ') state with the quantum numbers S_j and L_j as

$$\bar{A}_a\ (S_jL_jn\ell') = \frac{\sum_{SL}(2S+1)\ (2L+1)A_a(S_jL_jn\ell',\ SL)}{(2S_j+1)(2L_j+1)2\cdot\ (2\ell'+1)}\quad, \tag{11}$$

where the summation is over the resultant S and L for the configuration $\left[j(S_jL_j),\ n\ell'\right]$. Equation (11) assumes that all of the states $\left[j(S_jL_j),\ n\ell'\right]$ SL are populated according to their statistical weights, but it is not the case for low-density plasmas which are frequently encountered. It is convenient to introduce the quantity

$$B(n) = 2\omega_z(j)\sum_{\ell'}\frac{2\ell'+1}{1+A_r/\bar{A}_a(n\ell')} \tag{12}$$

Equation (12) assumes that the sum of the statistical weight of the state (j,n) is given by

$$\begin{aligned}\omega_{z-1}(n) &= \sum_{\ell',S,L}\omega_z(S_jL_jn\ell',SL)\\ &= \omega_z(S_jL_j)\sum_{\ell'}2(2\ell'+1)\end{aligned} \tag{13}$$

We make the following approximations that are valid for a large n,

$$\Delta E = E_{gj} - \frac{z^2 I_H}{n^2} \simeq E_{gj} \tag{14}$$

$$A_r^{z-1}(j,n\ell' \longrightarrow g,n\ell') \simeq A^z(j \rightarrow g) \tag{15}$$

With the assumptions of eqs. (11) - (15), equation (8) is rewritten as

$$\alpha^{tot} = \left(\frac{h^2}{2\pi mkT_e}\right)^{3/2} \sum_{jn} \frac{\omega_z(j)}{\omega_z(g)} A_r^z\,(j \longrightarrow g)$$

$$\times \sum_{\ell'} \frac{2\ell' + 1}{1 + A_r^z(j \longrightarrow g)/\bar{A}_a(j,n,\ell')} \cdot e^{-E_{gj}/kT_e}\,. \tag{16}$$

Here the transition probability is expressed as

$$\frac{\omega_z(j)}{\omega_z(g)} A_r^z(j \longrightarrow g) = \frac{8\pi^2 e^2 \nu^2}{mc^3} f_{gj} \tag{17}$$

where ν is the photon frequency and f_{gj} is the absorption oscillator strength. Burgess found that the results of his numerical calculations for various ions could be fitted to the formula

$$\alpha_d^{tot} = \frac{3 \times 10^{-3}}{T_e^{3/2}} f_{gj}\, A(x)\, B(z)\, \exp\left(-\frac{x\,C(z)}{T_e}\right) \text{cm}^3 s^{-1} \tag{18}$$

with

$$x \equiv E_{gj}/I_H(1 + z)$$

$$A(x) = x^{1/2}/(1 + 0.105x + 0.015x^2), \qquad x > 0.05 \tag{19}$$

$$B(z) = [z(1+z)^5/(z^2+13.4)]^{1/2}, \qquad z < 20 \tag{20}$$

$$C(z) = 1.58 \times 10^5 (1+z)/[1+0.015\, z^3/(1+z)^2], \quad \frac{xC}{T_e} < 5 \tag{21}$$

where T_e is in K. Later Burgess and Tworkowski[7] made a small correction: eq. (18) should be multiplied by the factor

$$D(z) = 0.84 + \frac{0.5}{(z+1)^2} + \frac{0.03(z-11)}{1 + 4.5 \times 10^{-5}(z-11)^3} \,. \tag{22}$$

3.2. Other formulas

On the basis of eq.(8) with eq. (7) various formulas have been devised besides eq. (18). In this section we list these formulas along with parameters to be employed in these formulas. We put emphasis on the total dielectronic recombination rate coefficient for a hydrogenic ion into a helium-like ion.

Tucker and Gould[8] propose the formula

$$\alpha_d^{tot} = \frac{1}{(k\,T_e)^{3/2}} \sum_j C_j \exp(-E_{gj} / k\,T_e) \tag{23}$$

and give the table of E_{gj} and C_j for several ionic species. In their treatment, however, they neglect the strong dependence of the autoionization probability on the angular momentum quantum number. Therefore, we put their result outside of our consideration.

Beigman et al.[3] begin with eq. (7) and divid the doubly excited levels into the two groups for which either the second term or the first term may be neglected in the last denominator. The approximate result for the total recombination rate coefficient is fitted by

$$\alpha_d^{tot} = C\left(\frac{E_{gj}}{kT_e}\right)^{3/2} \exp\left(- \frac{E_{gj}}{kT_e} \right) \qquad (24)$$

with

$$E_{gj} = \frac{3}{4} (z + 1)^2 I_H \qquad (25)$$

and C is expressed as $C=10^{-10}\,\bar{C}$, and $\bar{C}$ is given in fig. 3.

Ansari et al.[9] reproduce the general formula of Burgess in the form.

$$\alpha_d^{tot} = t^{-3/2} \sum_j F_j \exp\,(-P_j/t) \qquad (26)$$

with

$$t = 10^{-6}\, T, \quad (\mathrm{K}) \qquad (27)$$

and the parameters F_j and P_j are given in Table 1 for several low-lying states of j.

Aldrovandi and Pequignot[10] also adopt the general formula of Burgess together with appropriate atomic parameters. They gives the formula

$$\alpha_d^{-tot} = A_d T_e^{-3/2} \exp(-T_0/T_e)\,[1 + B_d \exp(-T_1/T_e)]\,, \tag{28}$$

where T's are in K and the parameters are given in Table 2.

Donaldson and Peacock[11] approximate eq. (7) neglecting the second term in the last denominator for $z+1 \leq 18$, and propose the following formula:

$$\alpha_d^{tot} = \frac{7.9 \times 1.0^{-12}}{(kT_e)^{3/2}} (z+1)^4 \theta(\Delta_z, n_t') \, \phi(\Delta_{z-1}, n_t'') \tag{29}$$

where kT_e is expressed in eV and

$$\Delta_z = (z+1)^2 I_H / kT_e \tag{30}$$

and

$$(n_t'')^{3.5} = 1.46 \times 10^6 \frac{z^2}{(z+1)^6} \tag{31}$$

The factors are expressed as

$$\theta(\Delta, n_t') = \sum_{n'=2}^{n_t'} f(n'\ell + 1 \rightarrow n\ell)$$

$$\times (1 - \frac{1}{n'^2})^2 \exp\{-\Delta[1 - \frac{1}{n'^2}]\} \tag{32}$$

$$\phi(\Delta, n_t'') = \sum_{n''=2}^{n_t''} \exp[\frac{\Delta}{(n'')^2}] \sum_{\ell=0}^{4} (2\ell + 1), \tag{33}$$

where the summation may be terminated at $n_t' = 4$. These factors are given in Tables 3 and 4. For heavier ions of $z+1 > 18$, the first term in the denominator of eq. (7) is neglected, and another formula is given

$$\alpha_d^{tot} = 3.16 \times 10^{-5} \frac{1}{(kT_e)^{3/2}} \frac{z^2}{(z+1)^2}$$

$$\times \beta(\Delta_z, n_t')\, \gamma(\Delta_{z-1}, n_t'') \qquad (34)$$

The recommended approximation is $n_t' = 4$ and $n_t'' = 10$.

$$\beta(\Delta, n_t') = \sum_{n'=2}^{n_t'} \frac{f(n'\ell+1 \longrightarrow n\ell)}{(1 - 1/n'^2)} \exp[-\Delta(1 - \frac{1}{n'^2})] \qquad (35)$$

$$\gamma(\Delta, n_t'') = \sum_{n''=2}^{n_t''} \frac{\exp(\Delta / n''^2)}{n''^3} \sum_{\ell''=1}^{n''} g_{\ell''+1}(\Delta E) \qquad (36)$$

The facters are given in Tables 5 and 6.

§4. Detailed calculations

So far we have been concerned with the approximate expressions for the total or overall dielectronic recombination rate coefficient. If we start with the individual dielectronic recombination process, eq. (7), and perform the summation, eq.(8), the resulting rate coefficient should be much more reliable. Such calculations should be made if we are interested in the population density of individual excited states of the helium-like ions. Several calculations have been made so far for the case of the present interest.

Shore[12] has used the configuration interaction method for the resonance collision processes of eq. (1) and has evaluated eq.(8) with an approximation for the ℓ-dependence of A_a. The resulting numerical value is given in the form

$$\alpha_d^{tot} = \frac{a_0}{T_e^{3/2}} \exp(-1.44\tilde{\nu}/T_e) \qquad (37)$$

where $\tilde{\nu}$ is the excitation energy in cm^{-1}, T_e is in K and a_0 is given in Table 7, where the correction by ref.7 has been applied.

Dubau[13] has performed close coupling calculations of dielectronic recombination for $He^+ \longrightarrow He$, $z = 1$. He considers the channels $(1s,\ell)$, $(2s,\ell)$, $(2p, \ell-1)$ and $(2p, \ell+1)$, and the long-range coupling potential connecting 2s and 2p has been diagonalized by using the quantum-defect theory. The resulting rate coefficient is shown in Fig.4.

For helium-like ions Dubau et al.[14] have calculated the satellite line intensity accompanying the hydrogenic resonance line. They consider the doubly excited configurations $2sn\ell$, $2pn\ell$, $3sn\ell$, $3pn\ell$, and $3d^2$. They evaluate the autoionization probability and stabilizing transition probability for each doubly excited states obtaining the satellite line intensities. The total dielectronic recombination rate coefficientr is given as the summation of these satellite line intensities. The result for Fe^{25+} (z=25) is shown in Fig.5.

Fujimoto and Kato,[15] in carrying out their program to calculate the excited state population densities of helium-like ions in high-temperature plasmas, have evaluated the dielectronic recombination to each excited states of helium-like ions. They assume the L-S coupling scheme for the doubly excited levels $2pn\ell$ and neglects the relativistic effects. For the low-lying levels of n=2 they employ the calculation by Boiko et al.[16] of the autoionization and stabilizing transition probabilities. For higher-lying levels the autoionization probability is evaluated using eq.(10') from the partial-wave collision strength given by Burgess et al.[17] The stabilizing transition probability is given the value of the spontaneous transition probability $2p \longrightarrow 1s$ of the hydrogen-like ion. The dielectronic recombination rate coefficient for individual excited level, eq. (7), is summed over 60 excited levels of $n<20$, and the contribution from the higher-lying levels of $n>20$ is estimated with an approximation to eqs. (7) and (10'). An example of the results for the individual dielectronic recombination rate coefficient is shown in Fig.6 for B^{3+} excited states. The total or overall dielectronic recombination rate coefficient is given in Figs. 7 and 8, for B^{4+} and Mg^{11+}, respectively. It is noted that this calculation includes only the stabilizing transition $2p \rightarrow 1s$ and underestimate the total recombination rate coefficient by 40% or less.

§ 5. Comparison

Various formulas described in § 3 are compared with more comprehensive calculations in § 4. We consider the cases of $z = 1$ ($He^{+} \longrightarrow He$), $z = 4$ ($B^{4+} \longrightarrow B^{3+}$), $z = 11$ ($Mg^{11+} \longrightarrow Mg^{10+}$) and $z = 25$ ($Fe^{25+} \longrightarrow Fe^{24+}$).

(i) $z = 1$ ($He^{+} \longrightarrow He$)

In Fig.4 various formulas are compared with the result by Dubau.[13] The revised version[7] of the general formula by Burgess gives extremely good agreement with Dubau. All of the other formulas give larger values by a factor of 2, but the disagreement is not so large.

(ii) $z = 4$ ($B^{4+} \longrightarrow B^{3+}$)

Various results are compared in Fig. 7. The general formula[7] gives good agreement with Fujimoto and Kato.[15] Others give larger values.

(iii) $z = 11$ ($Mg^{11+} \longrightarrow Mg^{10+}$)

Various results are compared in Fig. 8. The result is similar to the case of $z = 4$.

(iv) $z = 25$ ($Fe^{25+} \longrightarrow Fe^{24+}$)

Several results are presented in Fig.5. It should be noted that Dubau et al[14] and Fujimoto and Kato[15] are in good agreement. The general formula gives larger values.

§ 6. Limit of infinite z

We consider the z-dependence of $\sigma_{\bar{d}}$ of eq. (7). Roughly speaking, the probability A_r scales to z^4, and A_a does not have a z-dependence. The energy, of course, scales to z^2. Thus, in the limit of large z the situation is expected to become simple.

We assume the LS-coupling scheme is valid and neglect the relativistic effects. For $z \longrightarrow \infty$, equations (7) and (8) reduce to

$$\alpha_d^{tot} = \sum_{n,\ell'} Z_{2p,n\ell'} A_a(2p,n\ell'), \tag{38}$$

where we have included only the stabilizing transition $2p \longrightarrow 1s$. With the help of eq.(10), equation (38) is approximated to

$$(z+1)^3 \alpha_d^{tot} = \left(\frac{h^2}{2\pi m I_H} \right)^{3/2} \frac{1}{4} \Big\{ \sum_{\ell' SL} \omega_{He}(2p2\ell',{}^{2S+1}L)$$

$$\times A_a(2p2\ell',{}^{2S+1}L)\, \Theta^{-3/2} e^{-0.5/\Theta} + \frac{4I_H}{h} \frac{1}{2} (z+1)^2\, \Omega(1S \longrightarrow 2p)$$

$$[\Theta^{-1/2} (e^{-0.16/\Theta} - 1)\, e^{-0.75/\Theta}] \Big\} \tag{39}$$

with

$$\Theta = kT_e/(z+1)^2 I_H$$

Where I_H is in erg. We evaluate $A_a(2p2\ell',{}^{2S+1}L)$ from the partial-wave collision strength of ref. 17 and use its total collision strength for the second term. We obtain the numerical result

$$(z+1)^3 \alpha_d^{tot} = \left(\frac{h^2}{2\pi m I_H} \right)^{3/2} \frac{1}{4} \left\{ 2.67 \times 10^{15} Ⓗ^{-3/2} e^{-0.5/Ⓗ} \right.$$

$$\left. + 1.95 \times 10^{16} [Ⓗ^{-1/2} (e^{0.16/Ⓗ} - 1) e^{-0.75/Ⓗ}] \right\} \qquad (40)$$

The result is shown in Fig. 9.

A remarkable fact is that the first term that corresponds to the recombination through the intermediate states $2p2\ell'$ amounts to 3/5 of the total recombination rate. Furthermore, among these $2p2\ell'$ states $2p^2\ {}^1D_2$ state is the most important: almost 3/4 of the first term or a half of the total recombination is given from this state.

In Fig. 9 recombination rate coefficients for several cases of finite z are also reproduced: these are the results by Fujimoto and Kato as have been shown in Fig. 7, 8 and 5.

§7. Effects of finite electron and ion densities

Up to now we have assumed that the electron and ion densities are so low that the collisional effects are negligible on the doubly excited states as well as on the normal excited states of helium-like ion. The former effect would mix the autoionizing and closely-lying non-autoionizing states, thus increasing the recombination rate coefficient. It is also expected that electron collisions with the doubly excited-state ion would further excite the running electron before the core electron makes the stabilizing transition, thus reducing the recombination rate coefficient.

Jacobs et al.[18] have proposed that quasistatic micro-fields produced by plasma ions induce Stark mixing among the doubly excited states. This induces the autoionization probability to high-orbital angular momentum states that have negligible probability in the absence of the field. This results in an increase in the dielectronic recombination rate coefficient.

Population relaxation among the doubly excited levels due to electron collisions affects the dielectronic recombination. The effect of collisional transitions among $1s2\ell2\ell'$ levels of lithium-like ion has been considered,[19] and changes in the satellite line spectrum as well as in the dielectronic recombination rate have been predicted. The similar effect has been observed on the helium-like satellite spectrum emitted from the laser-produced plasma.[20]

Fujimoto and Kato[21] have proposed the dielectronic-capture-ladder-like excitation-ionization mechanism for the system of the doubly excited levels and evaluated its contribution to the 1s $\longrightarrow$ 2s and 1s $\longrightarrow$ 2p excitation rate coefficients. This mechanism involves the electron collisions on the doubly excited ions:i.e. the ladder-like excitation-ionization flow of electrons in the doubly excited Rydberg states results in the increase in excitation to singly excited levels. Its contribution has been found significant. This suggests that the dielectronic recombination rate coefficient for individual level, eq. (7), is reduced owing to this effect. The total recombination rate co-efficient, eq. (8), however, is hardly affected, because another effect sets in that reduces the effective recombination rate at still lower electron densities as described below.

We now consider the effect of electron collisions on the population density of the normal excited states of helium-like ion that are produced as a result of dielectronic recombinaion. eq. (1); If the collisional excitation takes place from this level before the electron decays radiatively to reach the ground state, dielectronic recombination is, in effect, interrupted, and the excited electron eventually returns to the continuum state with the hydrogenic ground-state ion. This process reduces the effective or total recombination rate coefficient. Several authors have evaluated the decrease in the recombination rate coefficient due to this effect; they consider the population density of the excited states and take into account the collisional and radiative processes by solving the rate equations by the method of the quasi-steady-state solution. Several examples of the result of calculation are given below for the n_e-dependence of the total recombination rate coefficient. In these calculations, besides the dielectronic recombination, radiative and three-body recombination into each of the levels are included; therefore the given quantities α_{CR} should be understood to correspond to the collisional-radiative recombination rate coefficient.

Burgess and Summers[22] have calculated the case of $He^+ \longrightarrow He$; Figure 10 shows their result. They also gives the changes in population density of the normal helium levels: Fig.11 shows an example corresponding to Fig.10. Fujimoto and Kato have applied their computer program to several cases of z, and their result are shown in Figs.12, 13 and 14 for z = 4, 11 and 25, respectively. The decrease in the rate coefficient with the increase in the electron density is due to the effective decrease in the dielectronic recombination, whereas the increase in the rate with the increase in the electron density in the low electron temperature regions is due to the combined effect of the three-body recombination and the collisional-radiative transitions.

Acknowledgments

The authors are indebted to Professor S. Hayakawa for his encouragements. They thank Professor Y. Itikawa for his interest in this study and valuable suggestions in completing the manuseript.

References

1. A. Burgess, Astrophys. J. 139 776(1964), 141 1588(1965).
2. M.J. Seaton and P.J. Storey, "Di-electronic recombination" in "Atomic Processes and Applications (ed., P.G. Burke and B.L. Moiseiwitsch) North-Holland 1976, p.133.
3. I.L. Beigman, L.A. Vainshtein and R.A. Syunyaev, Sov. Phys.-Uspekhi 11 411(1968).
4. V.L. Jacobs, J. Davis, P.C. Kepple and M. Blaha, Astrophys. J. 211 605(1977), 215 690(1977), M. Blaha, Astrophys. Letters 10 179(1972).
5. L.P. Presnyakov and A.M. Urnov, J. Phys. B 8 1280(1975).
6. M.A. Hayes and M.J. Seaton, J. Phys. B 11 L79(1978).
7. A. Burgess and A.S. Tworkowski, Astrophys. J. 205 L105(1976).
8. W.H. Tucker and R.J. Gould, Astrophy. J. 144 244(1966).
9. S.M.R. Ansari, G. Elwert and P. Mucklich, Z. Naturforsch. 25a 1781(1970).
10. S.M.V. Aldrovandi and D. Pequignot, Astron. & Astrophys. 25 137(1973).
11. T.P. Donaldson and N.J. Peacock, J. Quant. Spectr. Radiat. Transfer 16 599(1976).
12. B.W. Shore, Astrophys. J. 158 1205(1969).
13. J. Dubau, Ph.D.Thesis, Univ. of London (1973).
14. J. Dubau, A.H. Gabriel, M. Loulergue, L. Steenman-Clark and S. Volonte, Mon. Not. R. Astr. Soc. 195 705(1981)

15. T. Fujimoto and T. Kato, Astrophys.J. 246 994(1981), and unpublished calculations.

16. V.A. Boiko, A.Ya. Faenov, S.A. Pikuz and U.I. Safronova, Mon. Not. R. Astr. Soc. 181 107(1977).

17. A. Burgess, D.G. Hummer and J.A. Tully, Phil. Trans. Roy. Soc.A 266 225(1970).

18. V.L. Jacobs, J. Davis and P.C. Kepple, Phys. Rev. Letters 37 1390(1976).

19. V.L. Jacobs and M. Blaha, Phys. Rev. A21 525(1980).

20. V.I. Bayanov et al., JETP Letters 24 319(1976).

21. T. Fujimoto and T. Kato, Phys. Rev. Letters 48 1022(1982).

22. A. Burgess and H.P. Summers, Astrophys. J. 157 1007(1969).

Table 1

Parameter values for eq. (26). Ref.9

Excited state j / Ion	2p F	2p P	3p F	3p P	4p F	4p P
C VI	4.8(-11)	4.1	8.7(-12)	4.8	3.2(-12)	5.1
N VII	6.5(-11)	5.4	1.2(-11)	6.5	4.3(-12)	6.8
O VIII	8.5(-11)	7.0	1.5(-11)	8.3	5.4(-12)	8.8

Table 2

Parameter values for eq. (28). Ref. 10.

Ion	A_d ($cm^3\ s^{-1} {}^\circ K^{3/2}$)	T_0 (°K)	B_d	T_1 (°K)
He I	1.9(-3)	4.7(5)	0.3	9.4(4)
C V	4.8(-2)	4.1(6)	0.2	7.6(5)
N VI	6.6(-2)	5.4(6)	0.2	9.8(5)
O VII	8.6(-2)	7.0(6)	0.2	1.3(6)
Ne IX	1.3(-1)	1.1(7)	0.2	2.6(6)
Mg XI	1.7(-1)	1.5(7)	0.2	3.5(6)
Si XIII	2.1(-1)	2.0(7)	0.2	4.4(6)
S XV	2.5(-1)	2.5(7)	0.2	5.5(6)

Table 3 $\theta(\Delta, n_t')$

Parameter values for eq. (29). Ref. 11.

n_t' \ Δ	0.1	0.2	0.5	1.0	2.0	5.0	10.0
2	7.240-2	6.717-2	5.363-2	3.686-2	1.741-2	1.835-3	4.316-5
3	9.146-2	8.461-2	6.699-2	4.543-2	2.093-2	2.080-3	4.603-5
4	9.919-2	9.165-2	7.231-2	4.875-2	2.224-2	2.158-3	4.676-5
5	1.031-1	9.518-2	7.496-2	5.039-2	2.286-2	2.193-3	4.705-5
6	1.053-1	9.721-2	7.647-2	5.132-2	2.322-2	2.212-3	4.719-5
7	1.067-1	9.847-2	7.741-2	5.190-2	2.343-2	2.223-3	4.728-5
8	1.076-1	9.932-2	7.804-2	5.228-2	2.358-2	2.231-3	4.733-5
9	1.083-1	9.991-2	7.848-2	5.255-2	2.368-2	2.237-3	4.737-5
10	1.088-1	1.003-1	7.880-2	5.275-2	2.375-2	2.240-3	4.740-5

Table 4 $\phi(\Delta, n_t'')$

Parameter values for eq. (29). Ref. 11.

n_t'' \ Δ	0.1	0.2	0.5	1.0	2.0	5.0	10.0
2	4.101	4.205	4.533	5.136	6.595	1.396 + 1	4.873 + 1
3	1.320 + 1	1.341 + 1	1.405 + 1	1.519 + 1	1.784 + 1	2.965 + 1	7.607 + 1
4	2.226 + 1	2.252 + 1	2.333 + 1	2.477 + 1	2.803 + 1	4.195 + 1	9.288 + 1
5	3.129 + 1	3.159 + 1	3.251 + 1	3.414 + 1	3.778 + 1	5.294 + 1	1.063 + 2
6	4.032 + 1	4.064 + 1	4.164 + 1	4.340 + 1	4.730 + 1	6.328 + 1	1.182 + 2
7	4.934 + 1	4.968 + 1	5.073 + 1	5.258 + 1	5.667 + 1	7.325 + 1	1.292 + 2
8	5.835 + 1	5.871 + 1	5.980 + 1	6.172 + 1	6.596 + 1	8.298 + 1	1.398 + 2
9	6.736 + 1	6.773 + 1	6.886 + 1	7.083 + 1	7.518 + 1	9.255 + 1	1.499 + 2
10	7.637 + 1	7.675 + 1	7.790 + 1	7.992 + 1	8.436 + 1	1.020 + 2	1.599 + 2
11	8.538 + 1	8.576 + 1	8.694 + 1	8.900 + 1	9.351 + 1	1.114 + 2	1.697 + 2
12	9.439 + 1	9.478 + 1	9.597 + 1	9.806 + 1	1.026 + 2	1.207 + 2	1.793 + 2
13	1.034 + 2	1.038 + 2	1.050 + 2	1.071 + 2	1.117 + 2	1.300 + 2	1.889 + 2
14	1.124 + 2	1.128 + 2	1.140 + 2	1.162 + 2	1.208 + 2	1.392 + 2	1.983 + 2
15	1.214 + 2	1.218 + 2	1.230 + 2	1.252 + 2	1.299 + 2	1.484 + 2	2.077 + 2
16	1.304 + 2	1.308 + 2	1.321 + 2	1.342 + 2	1.390 + 2	1.576 + 2	2.171 + 2
17	1.394 + 2	1.398 + 2	1.411 + 2	1.433 + 2	1.481 + 2	1.668 + 2	2.264 + 2
18	1.484 + 2	1.488 + 2	1.501 + 2	1.523 + 2	1.571 + 2	1.759 + 2	2.357 + 2
19	1.574 + 2	1.578 + 2	1.591 + 2	1.613 + 2	1.662 + 2	1.850 + 2	2.449 + 2
20	1.664 + 2	1.668 + 2	1.681 + 2	1.703 + 2	1.752 + 2	1.941 + 2	2.542 + 2

Table 5 $\beta(\Delta, n_t')$

Parameter values for eq. (34). Ref. 11.

n_t' \ Δ	0.1	0.2	0.5	1.0	2.0	5.0	10.0
2	1.716-1	1.592-1	1.271-1	8.738-2	4.127-2	4.350-3	1.023-4
3	1.988-1	1.840-1	1.462-1	9.957-2	4.629-2	4.699-3	1.064-4
4	2.081-1	1.926-1	1.526-1	1.036-1	4.787-2	4.794-3	1.073-4
5	2.125-1	1.966-1	1.556-1	1.055-1	4.858-2	4.833-3	1.076-4
6	2.150-1	1.988-1	1.572-1	1.065-1	4.896-2	4.854-3	1.078-4
7	2.165-1	2.001-1	1.583-1	1.071-1	4.919-2	4.866-3	1.079-4
8	2.174-1	2.010-1	1.589-1	1.075-1	4.934-2	4.874-3	1.079-4
9	2.181-1	2.016-1	1.594-1	1.078-1	4.945-2	4.880-3	1.080-4
10	2.186-1	2.021-1	1.597-1	1.080-1	4.952-2	4.883-3	1.080-4

Table 6 $\gamma(\Delta, n_t'')$

Parameter values for eq. (34). Ref. 11.

n_t'' \ Δ	0.1	0.2	0.5	1.0	2.0	5.0	10.0
2	4.536-2	4.650-2	5.013-2	5.680-2	7.293-2	1.544-1	5.389-1
3	6.641-2	6.780-2	7.214-2	8.007-2	9.894-2	1.907-1	6.022-1
4	7.584-2	7.728-2	8.180-2	9.004-2	1.096-1	2.035-1	6.197-1
5	8.068-2	8.214-2	8.672-2	9.506-2	1.148-1	2.094-1	6.269-1
6	8.348-2	8.495-2	8.955-2	9.793-2	1.177-1	2.126-1	6.305-1
7	8.524-2	8.671-2	9.133-2	9.973-2	1.196-1	2.145-1	6.327-1
8	8.642-2	8.789-2	9.252-2	1.009-1	1.208-1	2.158-1	6.341-1
9	8.725-2	8.872-2	9.335-2	1.018-1	1.216-1	2.167-1	6.350-1
10	8.785-2	8.933-2	9.395-2	1.024-1	1.222-1	2.173-1	6.357-1
11	8.830-2	8.978-2	9.441-2	1.028-1	1.227-1	2.178-1	6.362-1
12	8.865-2	9.013-2	9.476-2	1.032-1	1.231-1	2.182-1	6.365-1
13	8.893-2	9.041-2	9.503-2	1.035-1	1.233-1	2.184-1	6.368-1
14	8.915-2	9.063-2	9.525-2	1.037-1	1.236-1	2.187-1	6.371-1
15	8.933-2	9.080-2	9.543-2	1.039-1	1.237-1	2.189-1	6.372-1
16	8.947-2	9.095-2	9.558-2	1.040-1	1.239-1	2.190-1	6.374-1
17	8.960-2	9.107-2	9.570-2	1.041-1	1.240-1	2.191-1	6.375-1
18	8.970-2	9.118-2	9.581-2	1.042-1	1.241-1	2.192-1	6.376-1
19	8.979-2	9.127-2	9.590-2	1.043-1	1.242-1	2.193-1	6.377-1
20	8.986-2	9.134-2	9.597-2	1.044-1	1.243-1	2.194-1	6.378-1

Table 7

Parameter values for eq. (37). Refs. 12 and 7.

Ion	$\tilde{\nu}(ji)$ cm^{-1}	$A^{rad}(ij)$ sec^{-1}	α_0
He^{+1}	3.29 (5)	1.0 (10)	2.8 (-3)
Li^{+2}	7.40 (5)	5.1 (10)	1.2 (-2)
Be^{+3}	1.32 (6)	1.6 (11)	2.6 (-2)
B^{+4}	2.06 (6)	3.9 (11)	4.7 (-2)
C^{+5}	2.96 (6)	8.1 (11)	7.6 (-2)
N^{+6}	4.03 (6)	1.5 (12)	1.1 (-1)
O^{+7}	5.26 (6)	2.6 (12)	1.4 (-1)

Figure Captions

Fig.1 Energy-level diagram pertinent to dielectronic recombinatoin. $X_z(j)$ denotes the z-times ionized ion in the singly excited state j. $X_{z-1}(j,n\ell')$ is the doubly excited ion with the core electron j, and the running electron $n\ell'$. A_a and r_d are, respectively, the autoionization probability and the dielectronic capture probability.

Fig.2 Schematic diagram of the excitation cross section σ_{ex}^{z} $(g \rightarrow j,\epsilon\ell)$ and the dielectronic capture cross section $\sigma_d(g \rightarrow j,n\ell)$.

Fig.3 The scale parameter for eq.(24) with $C=10^{-10}\,\overline{C}$. Ref.3.

Fig.4 Total dielectronic recombination rate coefficient for $He^+ \rightarrow He$. "Burgess" : eq.(18) with eq.(22). "Dubau" : ref.13. "Beigman" : eq.(24). "Aldrovandi & Pequignot" : eq.(28). "Shore" : eq. (37). "Donaldson & Peacock" : eq.(29).

Fig.5 Total dielectronic recombination rate coefficient for $Fe^{25+} \rightarrow Fe^{24+}$. "Burgess" : eq.(18) with eq.(22). "Dubau et al." : ref.14. "Donaldson & Peacock" : eq.(34). "Fujimoto and Kato" : ref.15.

Fig.6 Dielectronic recombination rate coefficient into individual excited level of B^{3+}. Ref.15.

Fig.7 Total dielectronic recombination rate coefficient for $B^{4+} \rightarrow B^{3+}$. "Burgess" : eq.(18) with eq.(22). "Fujimoto and Kato" : ref.15.

"Beigman" : eq.(24). "Shore" : eq.(37).
"Donaldson and Peacock" : eq.(29).

Fig.8 Total dielectronic recombination rate coefficient for $Mg^{11+} \rightarrow Mg^{10+}$. "Burgress" : eq.(18) with eq.(22). "Beigman" : eq.(24). "Donaldson and Peacock" : eq.(29). "Fujimoto and Kato" : ref.15.

Fig.9 Total dielectronic recombination rate coefficient for infinite nuclear charge, eq.(40). Several cases for finite z are also shown with the dotted curves as given by Fujimoto and Kato, ref.15.

Fig.10 Density dependence of the collisional-radiative recombination rate coefficient for $He^{+} \rightarrow He$. Ref.22.

Fig.11 Density dependence of the reduced population density of excited helium levels with the principal quantam number n. b_n is defined as $b_n = N(n)/N_E(n)$, where E denotes LTE(local thermodynamic equilibrium) as given by eq.(3).

Fig.12 Density dependence of the collisional-radiative recombination rate coefficient for $B^{4+} \rightarrow B^{3+}$. Ref.15.

Fig.13 Density dependence of the collisional-radiative recombination rate coefficient for $Mg^{11+} \rightarrow Mg^{10+}$. Ref.15.

Fig.14 Desity dependence of the collisional-radiative recombination rate coefficient for $Fe^{25+} \rightarrow Fe^{24+}$. Ref.15.

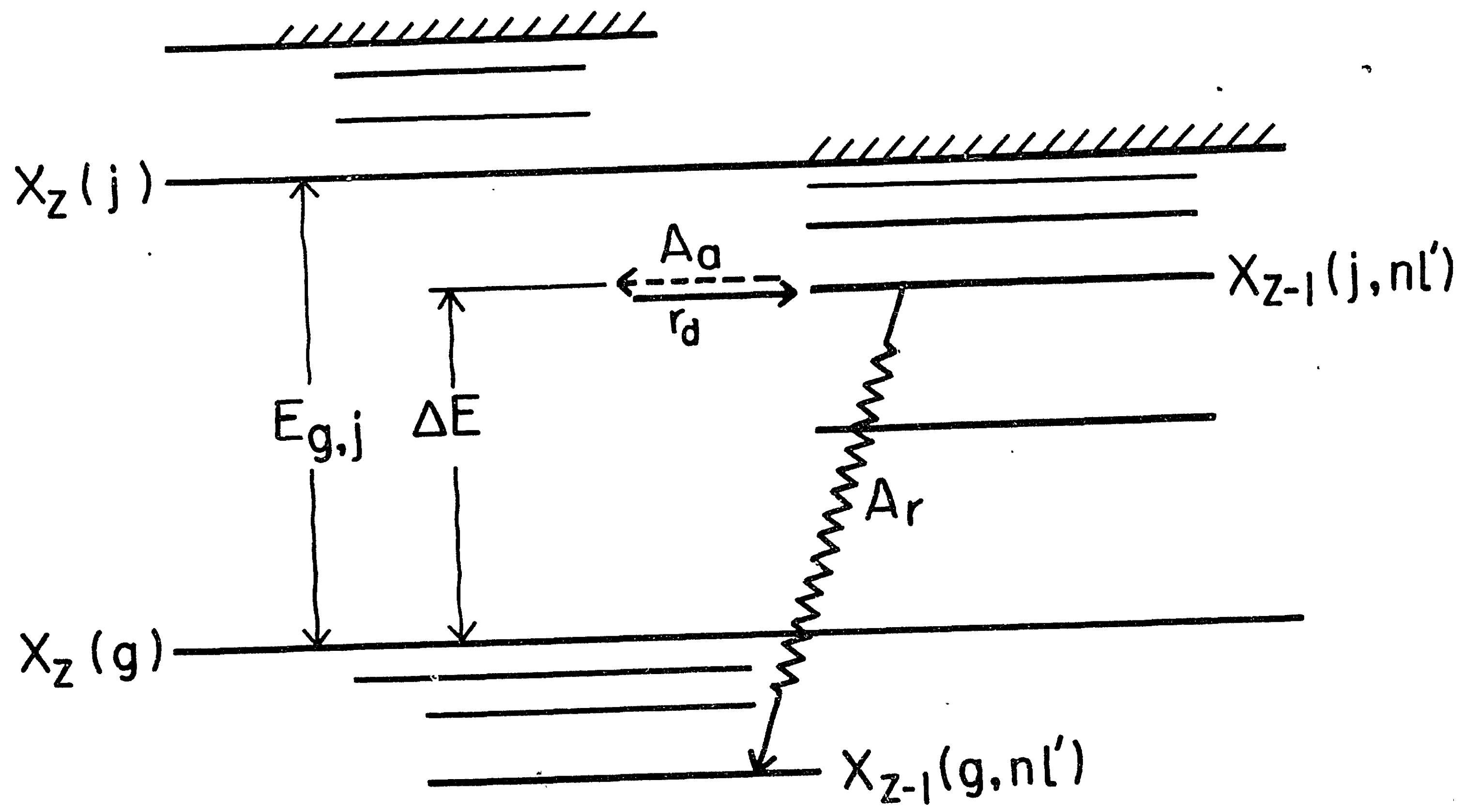

Fig. 1

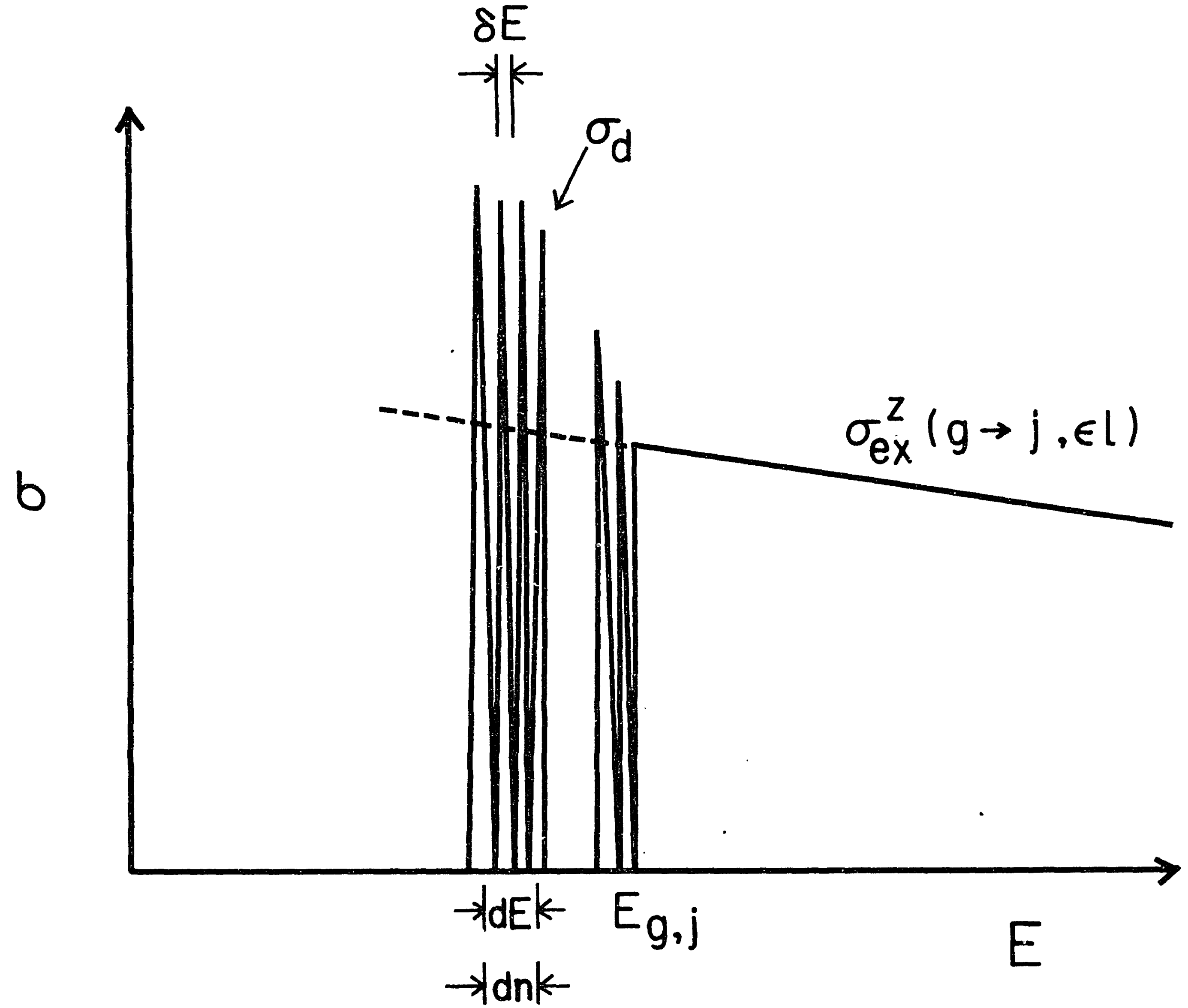

Fig. 2

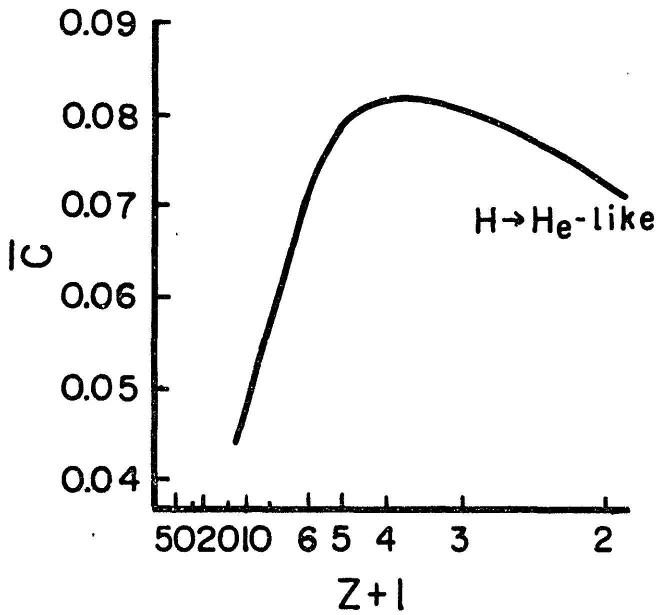

Fig. 3

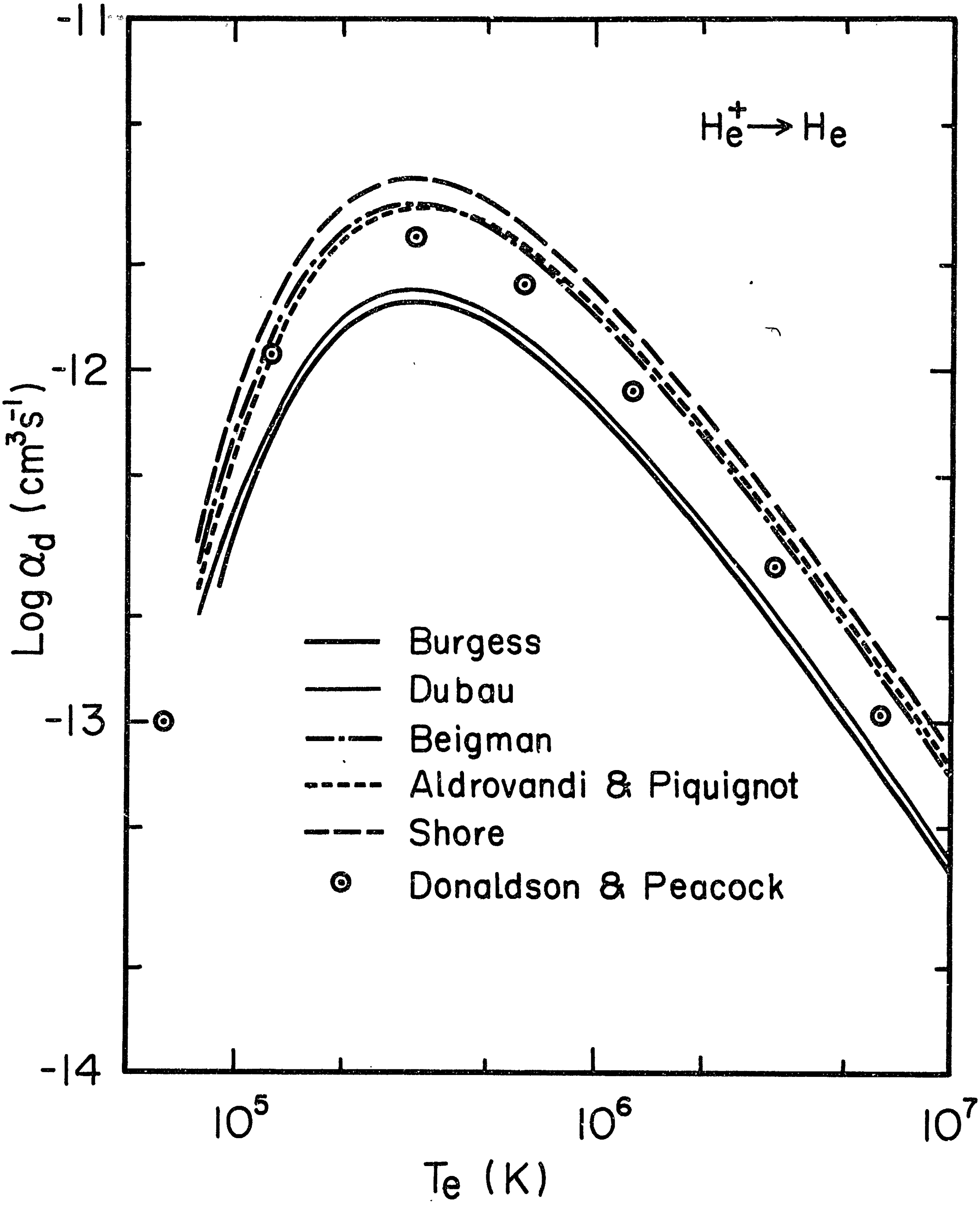
$He^{+} \rightarrow He$
Burgess
Dubau
Beigman
Aldrovandi & Piquignot
Shore
Donaldson & Peacock
-11
-12
-13
-14
Log α_d (cm^{3}s^{-1})
10^5
10^6
10^7
T_e (K)

Fig. 4

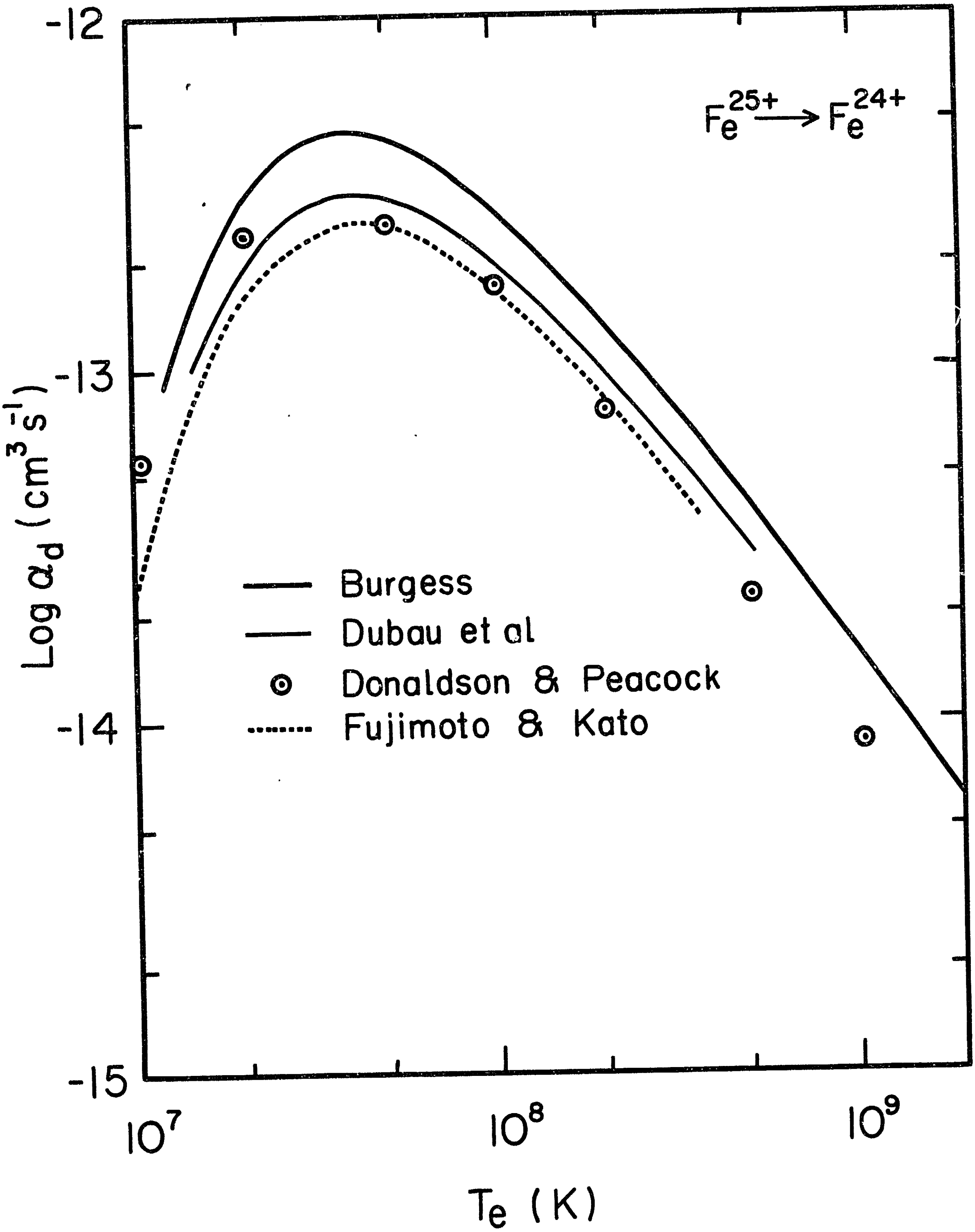

-12
-13
-14
-15
Log α_d ($cm^3 s^{-1}$)
$Fe^{25+} \longrightarrow Fe^{24+}$
Burgess
Dubau et al
Donaldson & Peacock
Fujimoto & Kato
10^7
10^8
10^9
T_e (K)

Fig. 5

Dielectronic Recombination Rate into BIV Excited Level

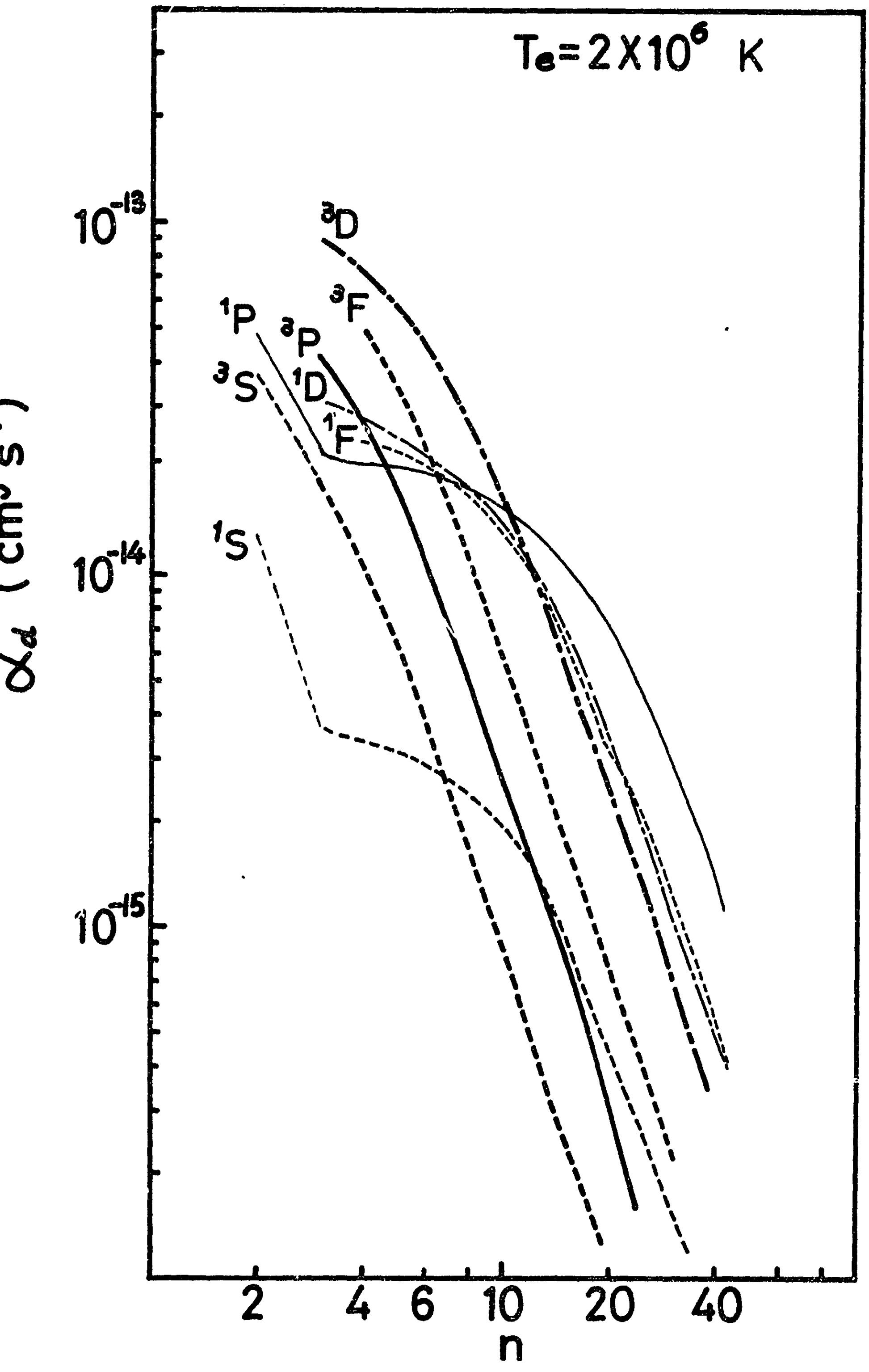

Fig. 6

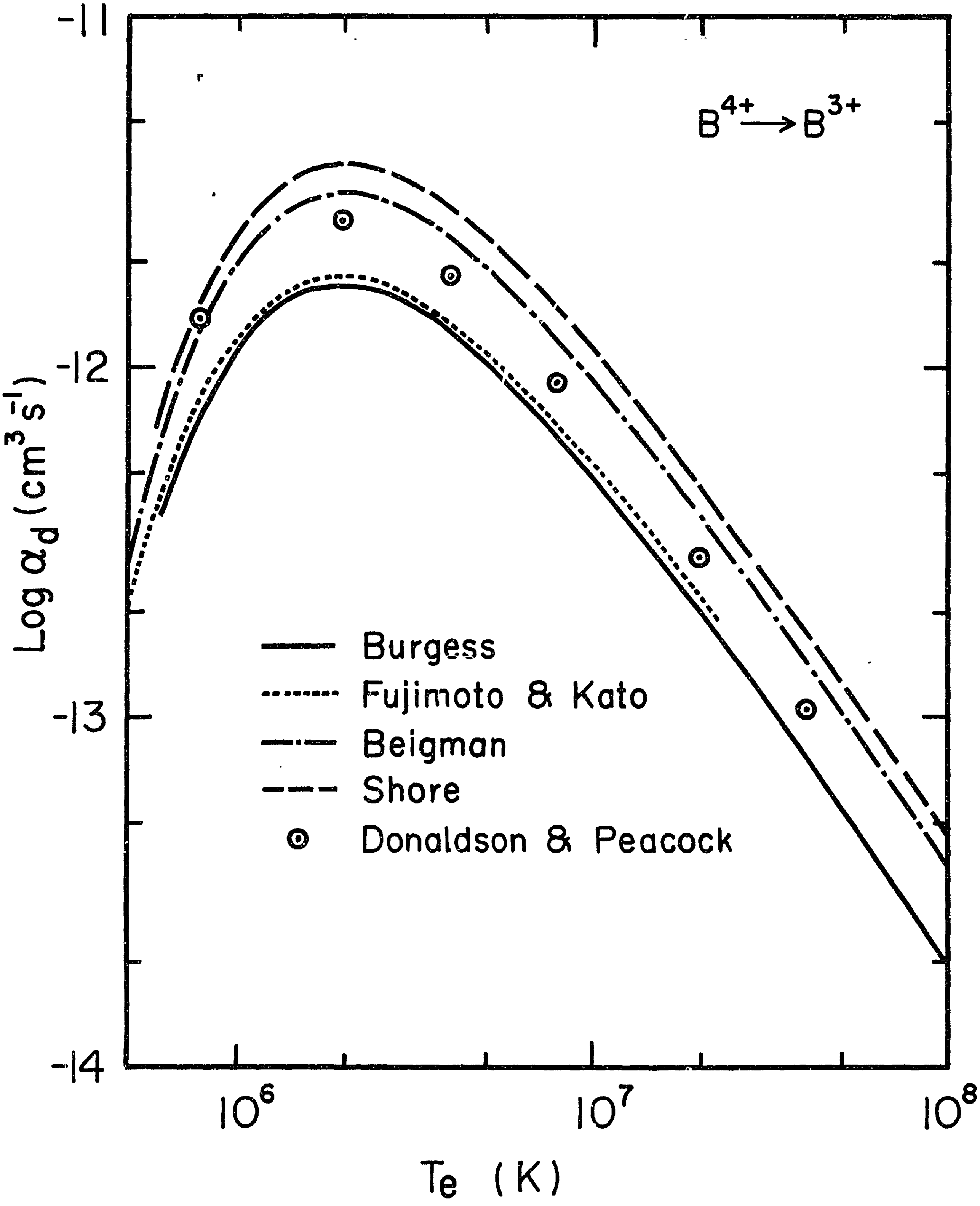

$B^{4+} \longrightarrow B^{3+}$
Burgess
Fujimoto & Kato
Beigman
Shore
Donaldson & Peacock
-11
-12
-13
-14
10^6
10^7
10^8
Log α_d ($cm^3 s^{-1}$)
Te (K)

Fig. 7

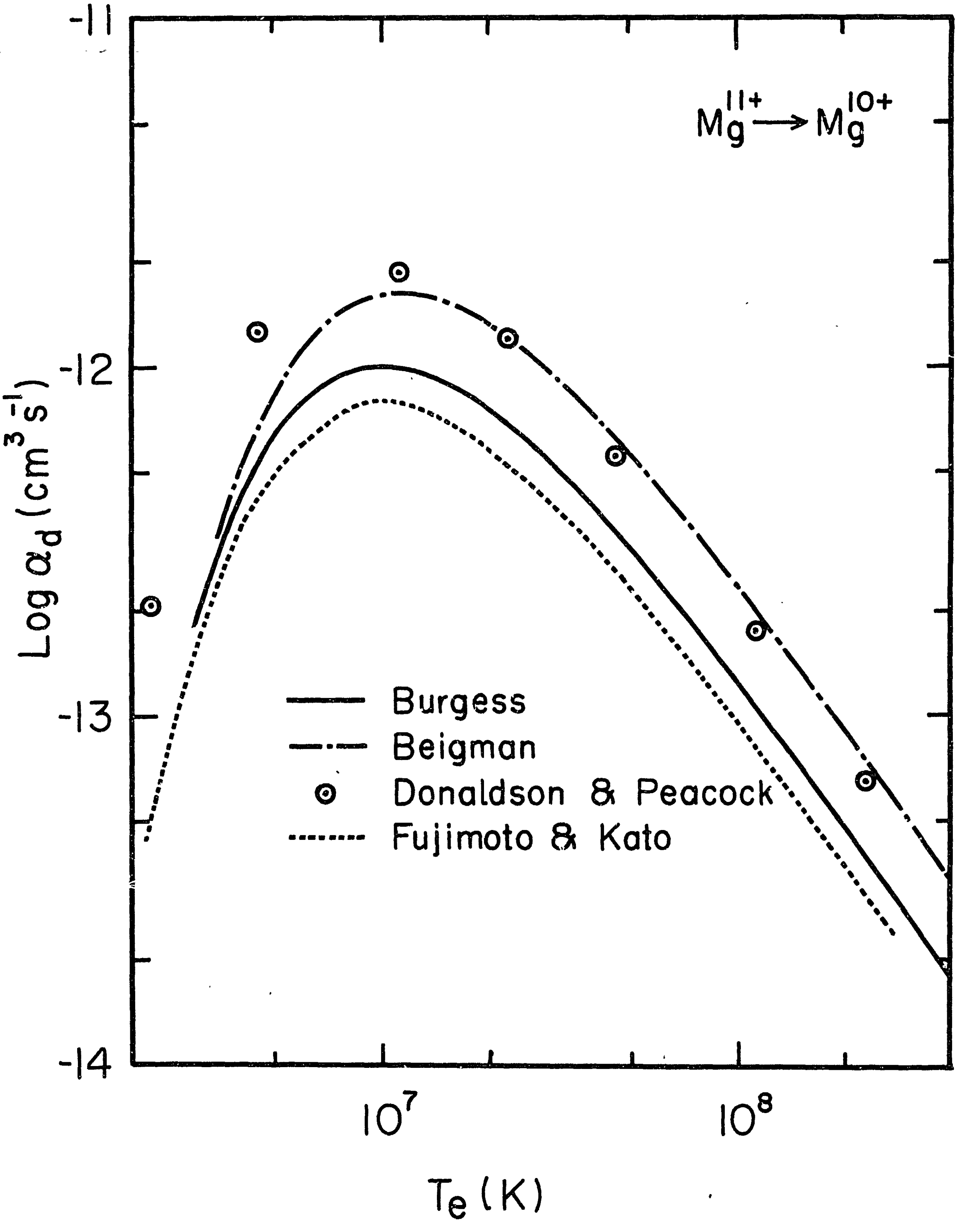

-11
-12
-13
-14
$Mg^{11+} \rightarrow Mg^{10+}$
Log α_d (cm^{3}s^{-1})
Burgess
Beigman
Donaldson & Peacock
Fujimoto & Kato
10^7
10^8
T_e (K)

Fig. 8

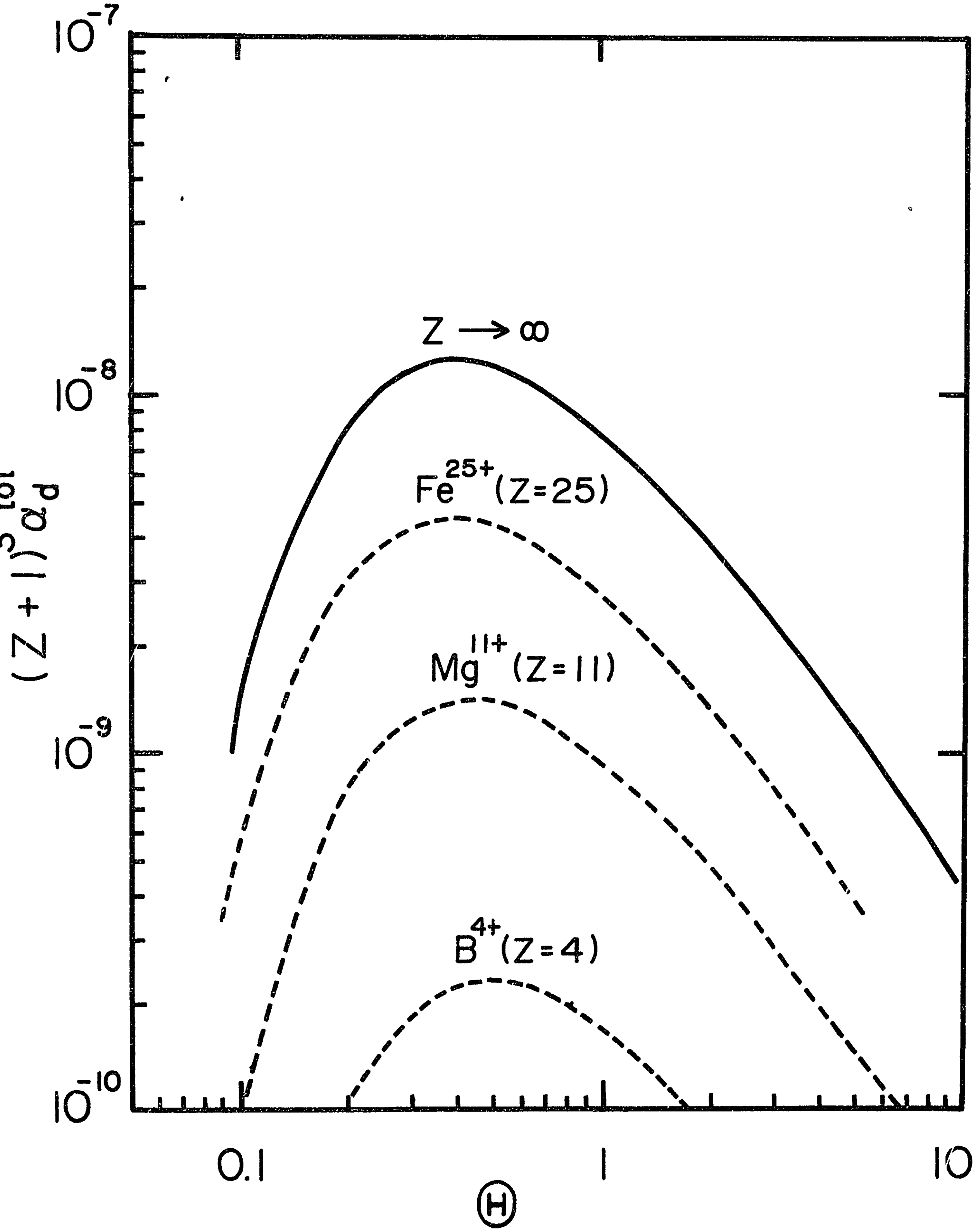

10^{-7}
10^{-8}
10^{-9}
10^{-10}
$(Z+1)^3 \alpha_d^{tot}$
$Z \longrightarrow \infty$
$Fe^{25+}(Z=25)$
$Mg^{11+}(Z=11)$
$B^{4+}(Z=4)$
0.1
1
10
Ⓗ

Fig. 9

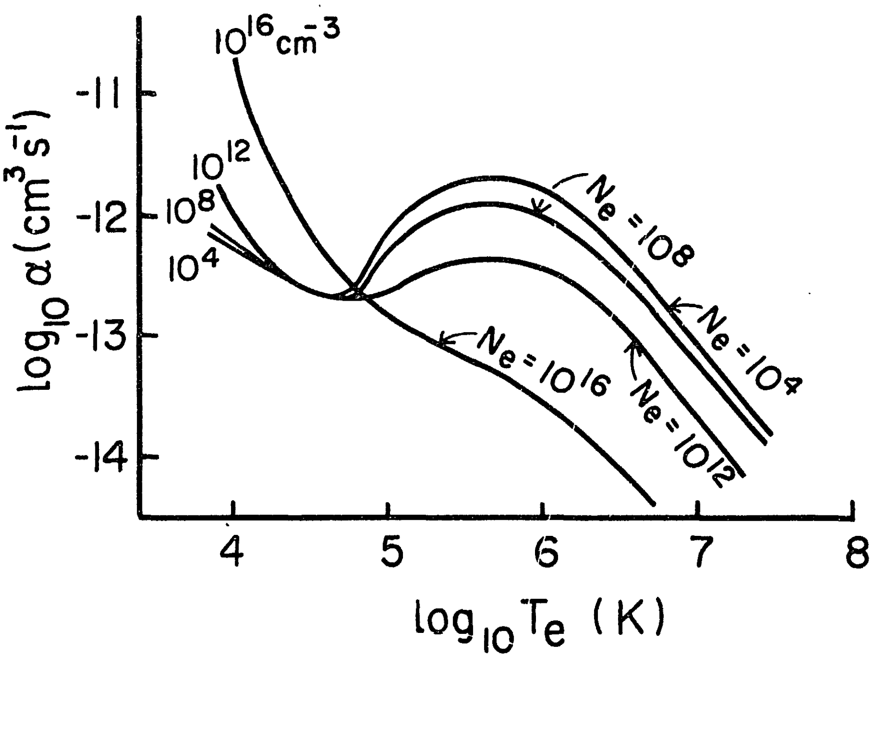
10^{16} cm^{-3}
10^{12}
10^{8}
10^{4}
-11
-12
-13
-14
$\log_{10} \alpha \, (cm^3 s^{-1})$
$N_e = 10^8$
$N_e = 10^4$
$N_e = 10^{12}$
$N_e = 10^{16}$
4
5
6
7
8
$\log_{10} T_e$ (K)

Fig. 10

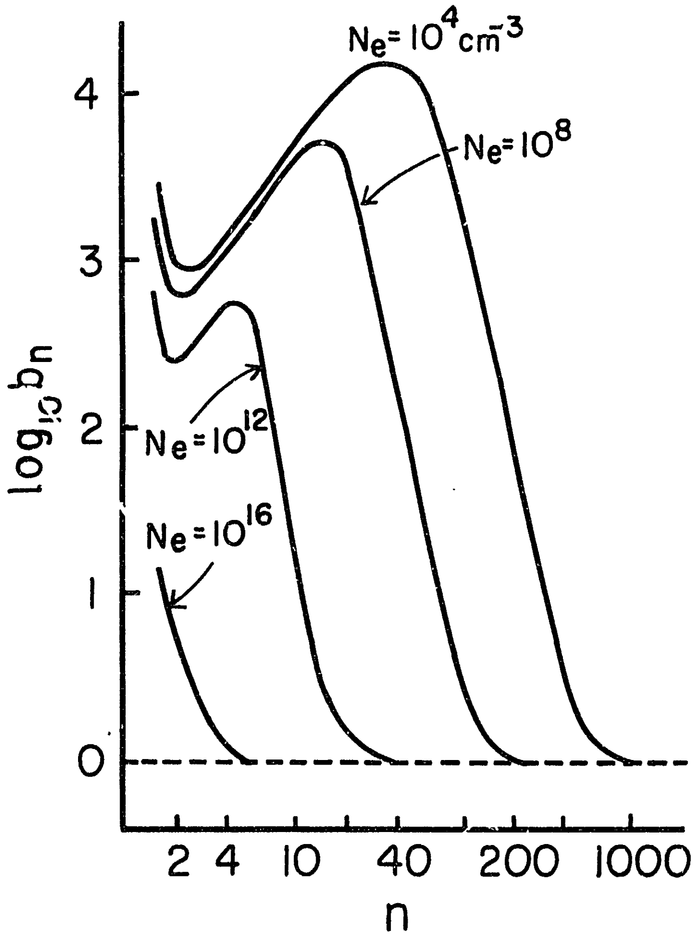

$N_e = 10^4 cm^{-3}$
$N_e = 10^8$
$N_e = 10^{12}$
$N_e = 10^{16}$
$\log_{10} b_n$
4
3
2
1
0
2 4 10 40 200 1000
n

Fig. 11

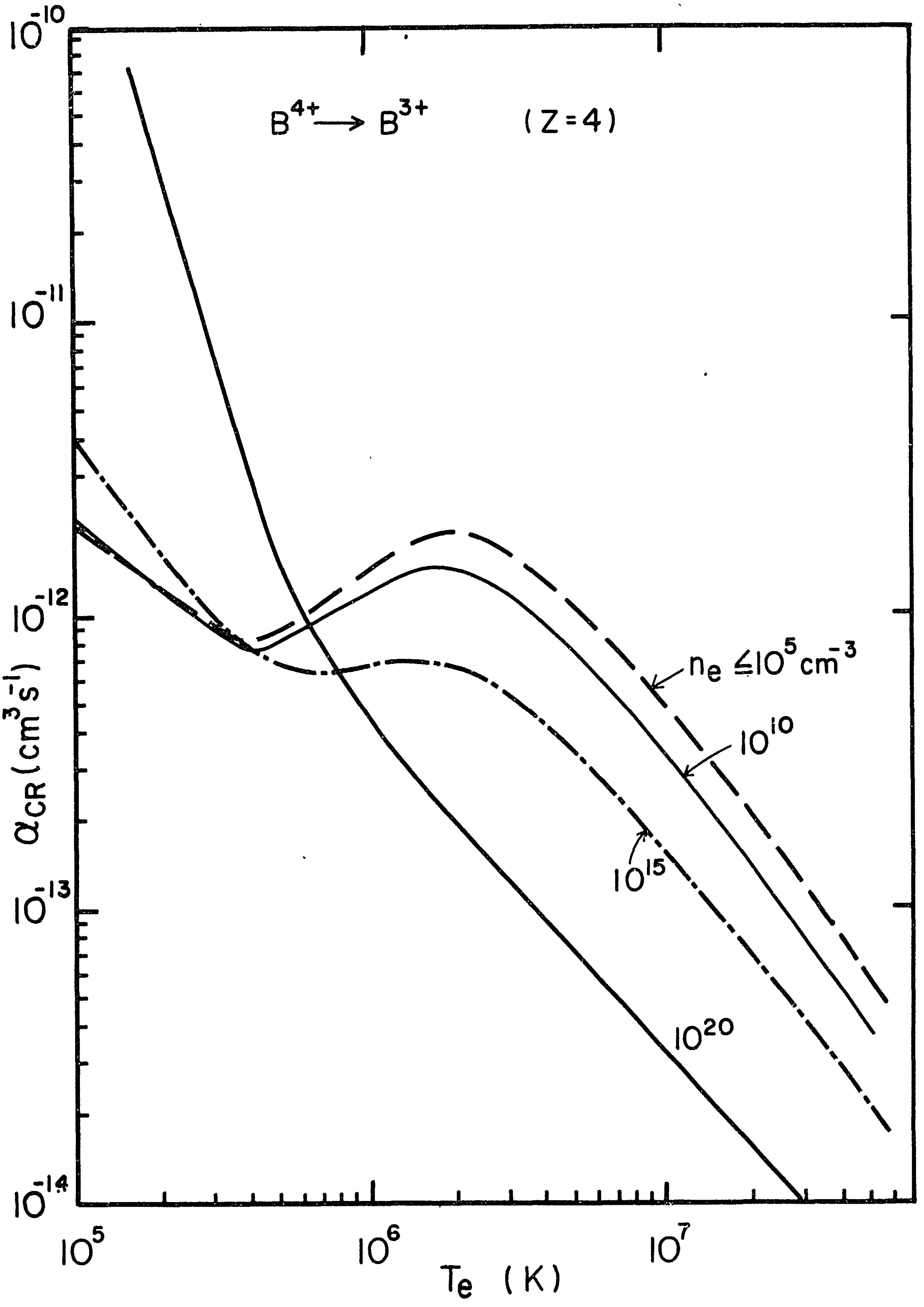

10^{-10}
10^{-11}
10^{-12}
10^{-13}
10^{-14}
$B^{4+} \longrightarrow B^{3+}$ (Z=4)
$n_e \leq 10^5 cm^{-3}$
10^{10}
10^{15}
10^{20}
α_{CR} ($cm^3 s^{-1}$)
10^5
10^6
10^7
T_e (K)

Fig. 12

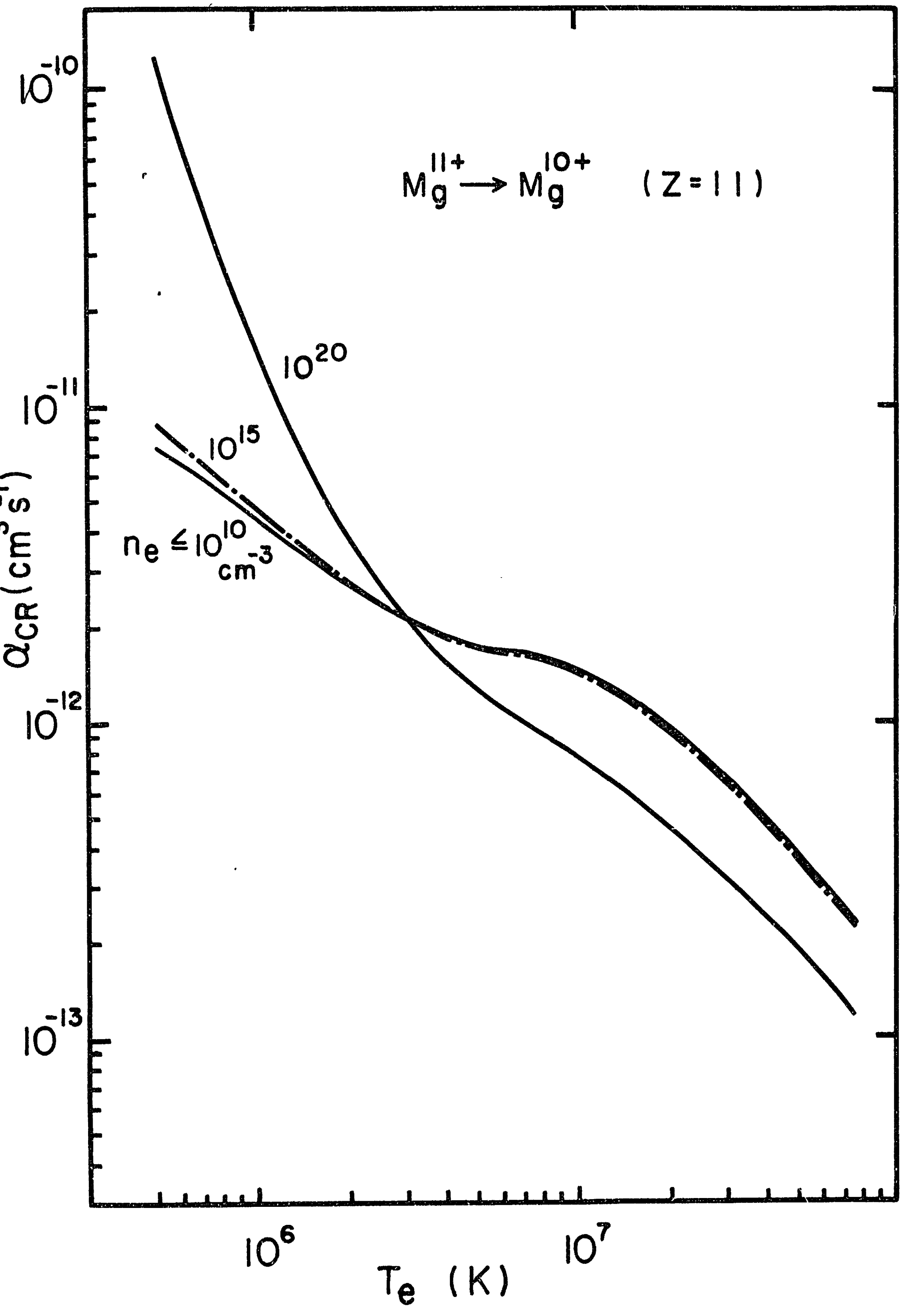
$Mg^{11+} \rightarrow Mg^{10+}$ (Z = 11)
10^{20}
10^{15}
$n_e \leq 10^{10}$ cm^{-3}
α_{CR} ($cm^3 s^{-1}$)
10^{-10}
10^{-11}
10^{-12}
10^{-13}
10^6
10^7
T_e (K)

Fig. 13

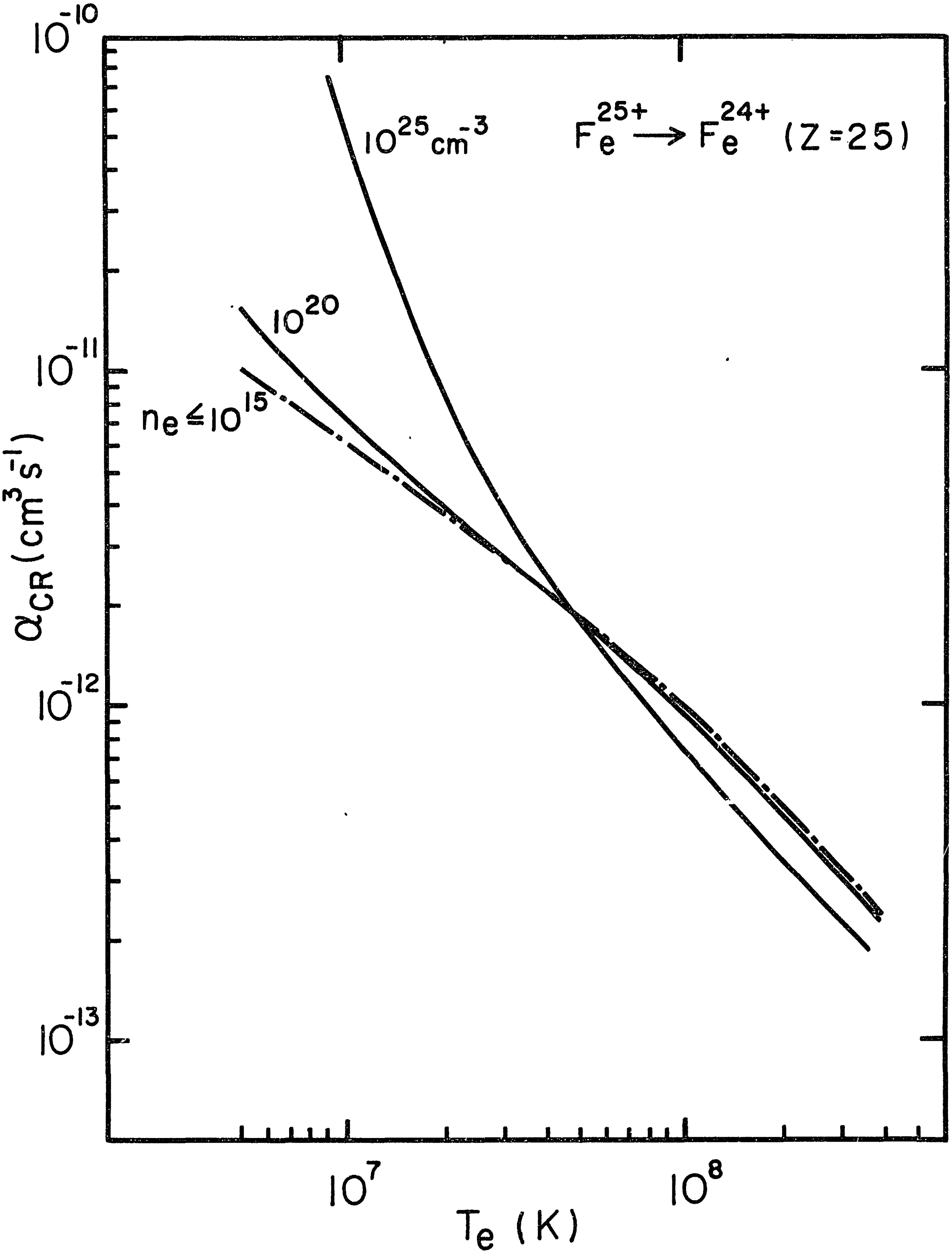

10^{-10}
10^{-11}
10^{-12}
10^{-13}
$10^{25}cm^{-3}$
$Fe^{25+} \rightarrow Fe^{24+}$ (Z=25)
10^{20}
$n_e \leq 10^{15}$
$\alpha_{CR}(cm^3 s^{-1})$
10^7
10^8
T_e (K)

Fig. 14

LIST OF IPPJ-AM REPORTS

IPPJ-AM-1*	"Cross Sections for Charge Transfer of Hydrogen Beams in Gases and Vapors in the Energy Range 10 eV–10 keV" H. Tawara (1977) [Published in Atomic Data and Nuclear Data Tables 22, 491 (1978)]
IPPJ-AM-2*	"Ionization and Excitation of Ions by Electron Impact –Review of Empirical Formulae–" T. Kato (1977)
IPPJ-AM-3	"Grotrian Diagrams of Highly Ionized Iron FeVIII-FeXXVI" K. Mori, M. Otsuka and T. Kato (1977) [Published in Atomic Data and Nuclear Data Tables 23, 196 (1979)]
IPPJ-AM-4	"Atomic Processes in Hot Plasmas and X-Ray Emission" T. Kato (1978)
IPPJ-AM-5*	"Charge Transfer between a Proton and a Heavy Metal Atom" S.Hiraide, Y. Kigoshi and M. Matsuzawa (1978)
IPPJ-AM-6*	"Free-Free Transition in a Plasma –Review of Cross Sections and Spectra–" T. Kato and H. Narumi (1978)
IPPJ-AM-7*	"Bibliography on Electron Collisions with Atomic Positive Ions: 1940 Through 1977" K. Takayanagi and T. Iwai (1978)
IPPJ-AM-8	"Semi-Empirical Cross Sections and Rate Coefficients for Excitation and Ionization by Electron Collision and Photoionization of Helium" T. Fujimoto (1978)
IPPJ-AM-9	"Charge Changing Cross Sections for Heavy-Particle Collisions in the Energy Range from 0.1 eV to 10 MeV I. Incidence of He, Li, Be, B and Their Ions" Kazuhiko Okuno (1978)
IPPJ-AM-10	"Charge Changing Cross Sections for Heavy-Particle Collisions in the Energy Range from 0.1 eV to 10 MeV II. Incidence of C, N, O and Their Ions" Kazuhiko Okuno (1978)
IPPJ-AM-11	"Charge Changing Cross Sections for Heavy-Particle Collisions in the Energy Range from 0.1 eV to 10 Mev III. Incidence of F, Ne, Na and Their Ions" Kazuhiko Okuno (1978)
IPPJ-AM-12*	"Electron Impact Excitation of Positive Ions Calculated in the Coulomb-Born Approximation –A Data List and Comparative Survey–" S. Nakazaki and T. Hashino (1979)
IPPJ-AM-13	"Atomic Processes in Fusion Plasmas – Proceedings of the Nagoya Seminar on Atomic Processes in Fusion Plasmas Sept. 5-7, 1979" Ed. by Y. Itikawa and T. Kato (1979)
IPPJ-AM-14	"Energy Dependence of Sputtering Yields of Monatomic Solids" N. Matsunami, Y. Yamamura, Y. Itikawa, N. Itoh, Y. Kazumata, S. Miyagawa, K. Morita and R. Shimizu (1980)

IPPJ-AM-15	"Cross Sections for Charge Transfer Collisions Involving Hydrogen Atoms" Y. Kaneko, T. Arikawa, Y. Itikawa, T. Iwai, T. Kato, M. Matsuzawa, Y. Nakai, K. Okuno, H. Ryufuku, H. Tawara and T. Watanabe (1980)
IPPJ-AM-16	"Two-Centre Coulomb Phaseshifts and Radial Functions" H. Nakamura and H. Takagi (1980)
IPPJ-AM-17	"Empirical Formulas for Ionization Cross Section of Atomic Ions for Electron Collisions –Critical Review with Compilation of Experimental Data–" Y. Itikawa and T. Kato (1981)
IPPJ-AM-18	"Data on the Backscattering Coefficients of Light Ions from Solids" T. Tabata, R. Ito, Y. Itikawa, N. Itoh and K. Morita (1981)
IPPJ-AM-19	"Recommended Values of Transport Cross Sections for Elastic Collision and Total Collision Cross Section for Electrons in Atomic and Molecular Gases" M. Hayashi (1981)
IPPJ-AM-20	"Electron Capture and Loss Cross Sections for Collisions between Heavy Ions and Hydrogen Molecules" Y. Kaneko, Y. Itikawa, T. Iwai, T. Kato, Y. Nakai, K. Okuno and H. Tawara (1981)
IPPJ-AM-21	"Surface Data for Fusion Devices – Proceedings of the U.S–Japan Workshop on Surface Data Review Dec. 14-18, 1981" Ed. by N. Itoh and E.W. Thomas (1982)
IPPJ-AM-22	"Desorption and Related Phenomena Relevant to Fusion Devices" Ed. by A. Koma (1982)
IPPJ-AM-23	"Dielectronic Recombination of Hydrogenic Ions" T. Fujimoto, T. Kato and Y. Nakamura (1982)

Available upon request to Research Information Center, Institute of Plasma Physics, Nagoya University, Nagoya 464, Japan, except for the reports noted with*.